Performance-Based Prediction Of Shear And Flexural Strengths Of Fiber-Reinforced Concrete Beams Using Machine Learning

Dr. M. Adil Khan[1] , Asjad Javed[2] , Naalain E Muhammad[3] , Manzoor Rahman[4], Afzal Siraj[5] , Zia Ullah[6] , Marjan Gul (Corresponding Author)[7] , Saad Zahid[8] , Sana Shahid[9] , Uzair Ali[10]

[1]Resident Engineer (RE), National Engineering Services Pakistan (NESPAK), Lahore, Pakistan adee.uol@gmail.com
[2]Communication and Works Department, Punjab, Pakistan asjad.javed58@gmail.com
[3]National University of Science and Technology (NUST), Islamabad, Pakistan imran61066@gmail.com
[4]Department of Civil Engineering, School of Civil and Environmental Engineering (SCEE), National University of Sciences and Technology (NUST), Islamabad, Pakistan manzoorrahman395@gmail.com
[5]School of Mechanics and Transportation Engineering, Northwestern Polytechnical University, Xi'an Shaanxi, 710072, China afzalsiraj@ymail.com
[6]University of Technology Nowshera (UoT), Nowshera, Pakistan ziaullahsaib@gmail.com
[7]Department of Civil Engineering, Balochistan University of Information Technology, Engineering and Management Sciences (BUITEMS), Quetta, Pakistan marjan.gul@buitms.edu.pk
[8]National University of Sciences and Technology (NUST), Quetta, Pakistan saady1231@hotmail.com
[9]Department of Civil Engineering, Abasyn University, Peshawar, Pakistan sanashahid6276@gmail.com
[10]Local Government and Rural Development Department, Khyber Pakhtunkhwa, Pakistan engruzair91@gmail.com

Abstract

Fiber-reinforced concrete (FRC) is an advanced construction material that enhances the tensile strength, ductility, and cracking resistance of conventional concrete. In this study, a database of 847 experimental tests compiled from the literature published between 1990 and 2025 was used to develop a machine-learning (ML) framework for predicting the shear and flexural strengths of FRC beams. The database spans various fiber types, fiber volume fractions (0.5–3.0%), concrete compressive strengths (20–120 MPa), and beam sizes and shapes. Six ML algorithms Artificial Neural Networks (ANN), Support Vector Regression (SVR), Random Forest (RF), Gradient Boosting Machines (GBM), Extreme Gradient Boosting (XGBoost), and an Adaptive Neuro-Fuzzy Inference System (ANFIS) were developed and evaluated using key material, geometric, and reinforcement parameters. Model performance was assessed using R^2, RMSE, MAE, and MAPE. XGBoost showed the highest predictive accuracy among all models, with $R^2 = 0.94$ for shear strength and $R^2 = 0.96$ for flexural strength, outperforming empirical and code-based prediction methods by up to 50% in mean absolute percentage error. Feature-importance analysis identified concrete compressive strength, fiber volume fraction, and reinforcement ratio as the dominant variables governing beam behaviour. The results demonstrate the capability of ML approaches to capture the complex nonlinear relationships governing FRC beam behaviour and indicate that the developed models can support strength prediction and design optimization with a high degree of reliability, contributing to safer, more economical, and more sustainable construction practice.

Keywords: Fiber-reinforced concrete; Machine learning; Shear strength; Flexural strength; Beam design; XGBoost; Design-code comparison.

1. Introduction

Concrete remains the most widely used human-made construction material globally, with annual production estimated at approximately 14 billion m^3, while global cement production is about 4.2 billion tonnes per year (GCCA, 2021). Despite its widespread application, conventional concrete exhibits inherent limitations, including low tensile strength, brittle failure behaviour, and limited crack resistance. These deficiencies are particularly critical in structural elements subjected to shear and flexural actions, such as beams, where cracking, stiffness degradation, diagonal tension failure, and sudden brittle failure may compromise structural integrity and safety (Dawood and Taher, 2023; Lantsoght, 2019; Nassif et al., 2024).

The incorporation of discrete fibers into the concrete matrix has emerged as an effective strategy for improving these limitations. Fiber-reinforced concrete (FRC), particularly steel fiber-reinforced concrete (SFRC), exhibits enhanced tensile resistance, ductility, energy absorption capacity, crack-bridging ability, and post-cracking behaviour (Nilimaa, 2023; Cui et al., 2022; Haq and Jia, 2026). Fibers bridge micro- and macro-cracks, redistribute tensile stresses, reduce crack propagation, and provide residual tensile capacity after matrix cracking. Consequently, the brittle failure mode of conventional concrete can be transformed into a more gradual and ductile structural response, especially in members governed by shear and flexural cracking (Lantsoght, 2019; Hassan et al., 2025).

The shear and flexural performance of FRC beams is governed by several interacting material, geometric, and reinforcement-related parameters. These include concrete compressive strength, beam width, effective depth, shear-span-to-depth ratio, longitudinal reinforcement ratio, stirrup configuration, fiber type, fiber volume fraction, fiber aspect ratio, fiber orientation, and post-cracking residual flexural strength (Rahman et al., 2021; Nassif et al., 2024; Hassan et al., 2025; Haq and Jia, 2026). Traditional design approaches generally rely on empirical or semi-empirical equations calibrated using limited experimental datasets. Although such models remain useful for practical design, they may not fully capture the nonlinear interactions among the governing variables, particularly when applied outside their original calibration ranges (ACI 544.4R-18, 2018; fib Model Code 2010, 2013; Lantsoght, 2019; Nassif et al., 2024).

Current empirical and code-based models for predicting the shear and flexural strengths of FRC beams are therefore associated with important limitations, including simplified assumptions, restricted applicability to specific parameter ranges, sensitivity to the experimental database used for calibration, and limited ability to account for fiber–matrix interaction and post-cracking behaviour (Lantsoght, 2019; Nassif et al., 2024; Haq and Jia, 2026). In addition, experimental characterization of FRC beams is time-consuming, costly, and highly dependent on test configuration, material variability, and loading conditions. These challenges highlight the need for more flexible and data-driven predictive frameworks capable of capturing complex structural behaviour with improved accuracy and efficiency.

Machine learning has emerged as a powerful computational approach for modelling complex nonlinear relationships in concrete materials and structural members. Unlike conventional regression-based equations, ML models can learn patterns directly from experimental databases and identify the relative influence of key input parameters on structural response (Rahman et al., 2021; Kang et al., 2021; Yaseen, 2023). Recent studies have demonstrated the effectiveness of artificial neural networks, support vector regression, Gaussian process regression, random forest, gradient boosting, XGBoost, gene expression programming, and explainable ML approaches for predicting the shear and flexural strengths of FRC, SFRC, and FRP-reinforced concrete beams (Nassif et al., 2024; Hassan et al., 2025; Haq and Jia, 2026). These methods offer strong nonlinear modelling capability, efficient pattern recognition, adaptability through the inclusion of new data, and rapid prediction once trained.

Accordingly, this study aims to develop and validate comprehensive machine-learning models for predicting the shear and flexural strengths of fiber-reinforced concrete beams. The specific objectives are: (i) to compile an extensive and diverse experimental database of FRC beam test results; (ii) to implement and compare six machine-learning algorithms for strength prediction; (iii) to identify the most influential parameters affecting shear and flexural strength through feature-importance analysis; (iv) to benchmark the predictive performance of the ML models against traditional empirical equations and code-based predictions; and (v) to develop a user-friendly predictive framework that can support practical design assessment and performance-based decision-making for FRC beams.

2. Literature Review

2.1 Fiber types and reinforcing mechanisms

Fiber-reinforced concrete incorporates discrete fibers distributed randomly throughout the concrete matrix. The most commonly used fiber types include steel fibers, with high tensile strength (1000–3000 MPa) and modulus of elasticity (~200 GPa), available in straight, hooked-end, crimped, and indented geometries (ACI 544.1R-18, 2018); synthetic fibers such as polypropylene, polyethylene, and polyvinyl alcohol, offering corrosion resistance and cost-effectiveness with a modulus of elasticity of 3–10 GPa (Neupane et al., 2025); alkali-resistant glass fibers, providing high tensile strength (2000–3500 MPa) suitable for thin-section applications though requiring careful durability consideration (Hussain & Yadav, 2023); and emerging natural fibers including sisal, jute, coir, and bamboo offering environmental benefits for non-structural applications (Sulochani et al., 2024).

Fibers enhance concrete performance through several mechanisms. Crack bridging occurs where fibers spanning a crack transfer tensile stresses across it, maintaining load-carrying capacity after matrix cracking (Cui et al., 2022). Crack arrestment occurs where fibers impede crack propagation by redistributing stress concentrations at crack tips, increasing fracture energy and toughness. Multiple cracking develops because, unlike plain concrete which exhibits localized failure — FRC develops distributed microcracking, enhancing ductility and energy absorption. Finally, post-cracking strength, provided by fibers after matrix cracking, is crucial for structural applications, particularly in shear-critical elements where diagonal tension cracks develop (Hussain & Yadav, 2023).

2.2 Conceptual comparison of FRC beam systems

Figure 1 summarizes, at a conceptual level, the typical relative shear- and flexural-strength enhancements, crack patterns, and post-cracking behaviour reported across the literature for conventional reinforced concrete (RC) beams compared with beams incorporating steel, synthetic, glass, natural, and hybrid fiber systems. The values shown are illustrative of general trends reported across the 1990–2025 literature and are not derived from the experimental database or the ML models developed in this study; they are presented here to orient the reader before the literature on shear and flexural mechanisms is discussed in detail. Section 4 (Results and Discussion) presents the data-driven findings of the present study.

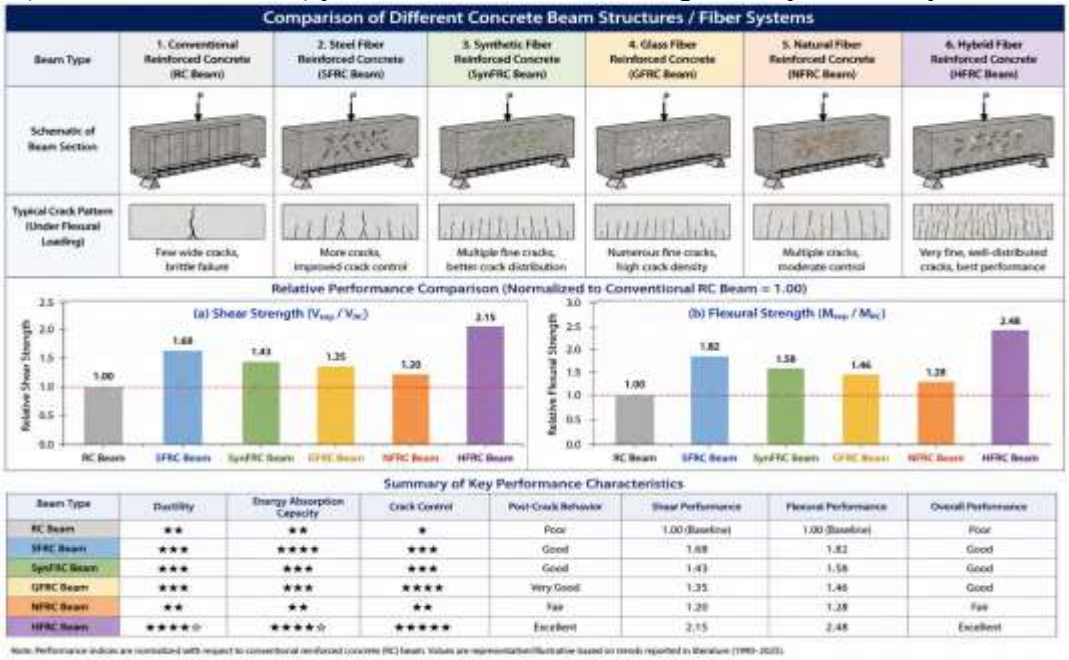

Fig. 1. Conceptual comparison of relative shear and flexural performance, crack patterns, and post-cracking behaviour reported in the literature for conventional and fiber-reinforced concrete beam systems. Values

are illustrative/representative of literature trends (1990–2025) and are not outputs of the ML models developed in this study.

2.3 Shear behaviour of FRC beams

The shear strength of reinforced concrete beams without stirrups derives from four primary components: the uncracked concrete compression zone resisting shear through diagonal compression; aggregate interlock, where rough crack surfaces transfer shear through interlocking aggregate particles; dowel action, where longitudinal reinforcement resists shear as cracks slide; and arch action in deep beams, where direct strut action transfers loads to the supports (Hwang et al., 2022). Fiber reinforcement enhances these mechanisms through improved aggregate interlock, as fibers crossing diagonal cracks maintain crack-surface contact and roughness, and crack-width control, which preserves aggregate-interlock effectiveness and protects reinforcement from corrosion (Cui et al., 2022). Fibers also provide direct shear resistance, as fibers oriented across potential shear cracks provide direct tensile resistance to diagonal tension, and enhance dowel action through crack-width control, which improves the effectiveness of longitudinal-reinforcement dowel action (Neupane et al., 2025).

Numerous experimental studies have investigated the shear behaviour of FRC beams. Abdallah et al. (2023) demonstrated that steel fibers could partially or completely replace conventional stirrups in beams with appropriate fiber volumes (1–2%). Rahman et al. (2021), compiling one of the larger SFRC shear databases reported in the literature (507 specimens), systematically examined the effects of fiber volume, aspect ratio, and concrete strength on shear capacity and demonstrated that boosting-type ensemble models outperform mechanics-based formulae for this problem. Hussain and Yadav (2023) compiled extensive test data and proposed modified shear-strength equations incorporating fiber influence through an empirical factor based on fiber geometry and volume. Zhang et al. (2023) performed comprehensive tests on high-strength FRC beams, revealing that fiber effectiveness diminishes at very high concrete strengths (>80 MPa) due to reduced fiber–matrix bond. Hwang et al. (2022) investigated post-cracking behaviour and residual-strength contributions, emphasizing the importance of fiber orientation and distribution. Recent studies by Huong et al. (2025) and Nilimaa (2023) explored hybrid fiber systems combining steel and synthetic fibers, demonstrating synergistic effects on shear performance and ductility.

2.4 Flexural behaviour of FRC beams

The flexural behaviour of FRC beams exhibits four distinct stages. In the pre-cracking stage, behaviour is linear-elastic, with both concrete and fibers contributing to stiffness, and the modulus of rupture typically exceeds that of plain concrete by 20–50%. In the cracking stage, initial flexural cracking occurs at loads below the ultimate capacity, and fibers immediately engage to bridge cracks, providing post-cracking strength. In the post-cracking stage, multiple cracking develops, fibers maintain tension stiffening, and the load–deflection response shows enhanced ductility and energy absorption. In the ultimate stage, failure occurs through concrete crushing in compression, fiber pull-out or rupture, or reinforcement yielding, depending on the reinforcement ratio and fiber content (ACI 544.4R-18, 2018).

Zedan Khalel et al. (2023) identified the key parameters affecting flexural performance. Fiber volume fraction: increasing fiber content generally enhances flexural strength and toughness up to an optimum level (typically 1.5–2.5%), beyond which workability issues and fiber balling reduce effectiveness. Fiber aspect ratio: higher aspect ratios improve fiber efficiency by increasing pull-out resistance, though very high ratios may cause mixing difficulties. Fiber orientation: random three-dimensional orientation in cast concrete provides isotropic reinforcement, though wall effects near formwork surfaces create preferential alignment (Abdallah et al., 2023). Concrete strength: higher matrix strength improves fiber–matrix bond but may reduce toughness if the matrix becomes too brittle. Reinforcement ratio: the interaction between conventional reinforcement and fibers affects failure mode and ductility, with fibers particularly beneficial in under-reinforced sections (Zedan Khalel et al., 2023).

2.5 Machine learning in concrete and FRC research

The application of machine learning to concrete technology dates to early work using artificial neural networks (ANNs) for predicting concrete compressive strength, with subsequent studies progressively incorporating ensemble and boosting methods (Yu et al., 2025). Lee et al. (2023) compared multiple ML algorithms for high-performance-concrete strength prediction and found that ensemble methods outperformed individual models. Chen et al. (2022) developed ANN and SVR models for fiber-reinforced-concrete-related compressive-strength prediction, achieving R^2 values exceeding 0.95. Cui et al. (2022) reviewed ML applications relevant to fire engineering and structural performance of fiber composites, and Neupane et al. (2025) examined data-driven approaches relevant to structural health monitoring of concrete elements.

Closer to the present study, Rahman et al. (2021) developed eleven ML models including linear and regularized regressions, tree-based ensembles, SVR, ANN, and XGBoost to predict the shear capacity of steel-fiber-reinforced concrete (SFRC) beams from a 507-specimen database, finding XGBoost to be the most accurate and identifying shear span-to-depth ratio, longitudinal reinforcement ratio, concrete strength, and fiber volume fraction as the most influential parameters. Yu et al. (2022) likewise evaluated several artificial-intelligence models for the shear capacity of SFRC beams without stirrups. A 2023 study in Case Studies in Construction Materials compared XGBoost, LightGBM, and gene-expression programming for the shear strength of synthetic-FRC deep beams, finding boosting methods ($R^2 \approx 0.95–0.98$) substantially more accurate than the ACI 318-19 design equation ($R^2 \approx 0.76$) and proposing a closed-form GEP model for design use.

Despite this progress, several gaps remain in ML applications for FRC beams: (i) many studies focus on compressive strength or isolated properties, with relatively few addressing shear and flexural strengths of beams simultaneously; (ii) many studies use small, homogeneous datasets (<200 samples), limiting generalizability; (iii) systematic comparison of multiple ML algorithms on a common, large, heterogeneous FRC-beam database remains limited; (iv) interpretability e.g., via SHAP-based feature-importance analysis is not yet standard practice across this literature; and (v) user-friendly tools integrating ML models with existing design frameworks remain scarce. The present study addresses these gaps through the development of validated ML models for FRC beam shear- and flexural-strength prediction based on an extensive, heterogeneous experimental database.

3. Database and Methodology

The overall workflow of the study database compilation, preprocessing, development of six ML models, validation, and packaging into a prediction tool is summarized in Figure 2.

Fig. 2. Machine learning framework adopted for FRC beam shear- and flexural-strength prediction.

3.1 Database compilation

A comprehensive experimental database was compiled through an extensive literature review of peer-reviewed journal articles, conference proceedings, and technical reports published between 1990 and 2025. The inclusion criteria were defined to ensure consistency and reliability of the dataset. Only experimental tests on simply supported fiber-reinforced concrete (FRC) beams subjected to monotonic loading were

considered. The selected specimens were required to have complete information on material properties, fiber characteristics, beam geometry, reinforcement details, and measured shear or flexural capacity. In addition, the database was limited to beams without conventional shear reinforcement or beams in which fibers acted as the primary shear-resisting mechanism. The concrete compressive strength was restricted to 20–120 MPa, and the fiber volume fraction was limited to 0.5–3.0%.

Specimens were excluded when conventional stirrups were used in combination with fibers, when loading was dynamic or cyclic, when essential material or geometric parameters were missing, or when the reported results were identified as physically inconsistent or clear statistical outliers.

After applying these selection criteria, the final database consisted of 847 experimental beam tests collected from 127 published studies. The database covers a broad range of concrete strengths, fiber properties, beam dimensions, reinforcement ratios, and strength responses, making it suitable for developing and validating machine-learning models for both shear and flexural strength prediction. The statistical distribution of the main input and output variables is summarized in Table 1.

Table 1. Statistical summary of the compiled experimental database.

Parameter	Range	Mean	Unit
Concrete compressive strength	22.5–118.0	52.3	MPa
Splitting tensile strength	2.1–8.9	4.2	MPa
Elastic modulus	22.0–48.5	32.1	GPa
Fiber volume fraction	0.5–3.0	1.35	%
Fiber length	13.0–60.0	32.4	mm
Fiber diameter	0.15–1.20	0.52	mm
Fiber aspect ratio	30–120	64.5	—
Beam width	100–300	152.3	mm
Effective depth	150–550	285.4	mm
Span	600–3000	1420.5	mm
Shear span-to-depth ratio	1.5–6.0	3.2	—
Tension reinforcement ratio	0.8–3.5	1.85	%
Ultimate shear strength	1.8–8.9	3.82	MPa
Ultimate flexural strength	12.5–285.0	78.4	kN·m

Concrete compressive strength in the compiled database ranged from 22.5 to 118.0 MPa, while the fiber volume fraction varied from 0.5 to 3.0%. The database also covers a wide range of beam geometries, with effective depths between 150 and 550 mm and shear span-to-depth ratios between 1.5 and 6.0. The ultimate shear strength ranged from 1.8 to 8.9 MPa, whereas the ultimate flexural strength varied from 12.5 to 285.0 kN·m. The distribution of fiber types is summarized in Table 2 and illustrated in Figure 2, showing that steel fibers represent the largest portion of the database, followed by synthetic, glass, and natural fibers.

Table 2. Fiber-type distribution in the database

Fiber type	Number of tests	Percentage
Steel fibers	612	72.3%
Synthetic fibers	158	18.6%
Glass fibers	52	6.1%
Natural fibers	25	3.0%
Total	847	100%

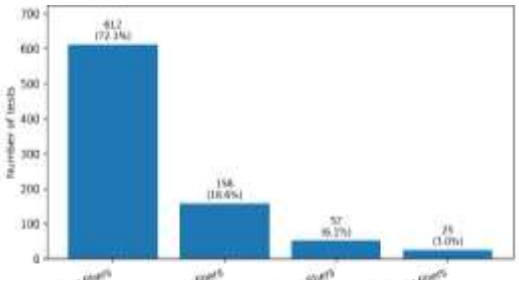

Fig. 3. Fiber-type distribution of the compiled FRC beam database.

3.2 Input and output variables

Table 3 summarizes the input and output variables used for model development. Input variables include concrete compressive strength (converted to equivalent cylinder strength where reported as cube strength), fiber volume fraction, fiber aspect ratio, fiber type (one-hot encoded), beam width, effective depth, shear span-to-depth ratio, tension reinforcement ratio, concrete elastic modulus, and maximum aggregate size. Output variables are the ultimate shear strength, $V_{u,max}/(bxd)$, in MPa, and the ultimate flexural strength (maximum moment capacity) in kN·m.

Table 3. Input and output variables used for model development.

Category	Variables
Input Variables	Concrete compressive strength, fiber volume fraction, fiber aspect ratio, fiber type, beam width, effective depth, shear span-to-depth ratio, reinforcement ratio, elastic modulus, aggregate size
Output Variables	Ultimate shear strength (MPa), ultimate flexural strength (kN·m)

3.3 Data preprocessing

Data preprocessing comprised rigorous cleaning: records with missing critical parameters were excluded (23 tests removed); statistical outliers beyond ±3 standard deviations were investigated, and 12 tests with clear reporting errors were removed; and physical-plausibility checks were applied to all remaining records. Input variables were normalised to the [0, 1] range using min–max scaling to prevent variables with larger magnitudes from dominating the learning process. Fiber type was one-hot encoded to avoid implying an ordinal relationship among categories. The dataset was randomly partitioned into a training set (677 samples, 80%) for model training and hyperparameter tuning, and a testing set (170 samples, 20%) for final evaluation, with stratified sampling to ensure similar distributions of fiber type and strength range in both subsets, and a fixed random seed (seed = 42) for reproducibility.

3.4 Machine learning algorithms

Six machine-learning algorithms were selected based on their demonstrated performance in structural-engineering applications and their ability to capture nonlinear relationships. Table 4 summarizes the architecture, key hyperparameters, and software implementation of each algorithm; full descriptions follow.

Table 4. Machine learning algorithm configurations.

Algorithm	Architecture / approach	Key hyperparameters	Software
ANN	Feedforward multilayer perceptron, backpropagation; input layer (10 neurons), two hidden layers (15 and 8 neurons), output layer (1 neuron); ReLU activation (hidden), linear activation (output)	Levenberg–Marquardt training; L2 regularisation $\lambda = 0.001$; 500 epochs, early-stopping patience = 50; batch size 32; learning rate 0.001 (adaptive); MSE loss; Adam optimiser	TensorFlow 2.8 / Keras
SVR	Support Vector Regression with RBF kernel; ε-insensitive loss; kernel trick for nonlinear regression without explicit high-dimensional mapping	$C = 100$; $\varepsilon = 0.01$; $\gamma = 0.05$; tolerance = 0.001	scikit-learn 1.0

Random Forest	Bagged ensemble of decision trees with feature-subset randomisation at each split, reducing variance without increasing bias	200 trees; max depth 25; min samples/split 5; min samples/leaf 2; max features = √n; bootstrap = True; random_state = 42	scikit-learn
GBM	Sequential ensemble of weak learners (decision trees), $F(x) = \Sigma \beta m \cdot hm(x)$, fitted via gradient descent in function space; Huber loss for robustness to outliers	150 estimators; learning rate 0.1; max depth 5; subsample 0.8; min samples/split 10; Huber loss	scikit-learn
XGBoost	Regularised gradient boosting with second-order gradient information, sparsity-aware splitting, and parallelised tree construction; $Obj(\theta) = \Sigma L(yi, \hat{y}i) + \Sigma \Omega(fk)$, $\Omega(fk) = \gamma T + 0.5\lambda\|w\|^2$	Bayesian-optimised: 300 estimators; learning rate 0.05; max depth 7; subsample 0.85; colsample_bytree 0.9; min_child_weight 3; $\gamma = 0.1$; $\lambda = 1.0$; $\alpha = 0.5$; random_state = 42; early-stopping rounds = 50	XGBoost (Python)
ANFIS	Sugeno-type fuzzy inference, 5-layer architecture (fuzzification, rule firing, normalisation, defuzzification, summation); rules of the form "If (x1 is A1) and (x2 is B1) then f1 = p1x1 + q1x2 + r1" with Gaussian membership functions	3 Gaussian membership functions per input; rules reduced to 50 via clustering; hybrid learning, 200 epochs; initial step size 0.01, decrease rate 0.9, increase rate 1.1	Custom Python

3.5 Hyperparameter optimization and cross-validation

Hyperparameters were tuned using Bayesian optimisation with Gaussian-process surrogate models. The procedure defined a parameter search space for each algorithm, initialised with 20 random samples, iteratively selected promising parameter combinations using the Expected Improvement acquisition function, evaluated each candidate using 5-fold cross-validation on the training set, updated the surrogate model, and repeated for 100 iterations, selecting the parameters that maximised cross-validation R^2. Five-fold stratified cross-validation was used throughout to obtain robust performance estimates and reduce the risk of overfitting.

3.6 Performance evaluation metrics

Model performance was assessed using: the coefficient of determination, $R^2 = 1 - \Sigma(yi - \hat{y}i)^2 / \Sigma(yi - \bar{y})^2$; the root mean square error, $RMSE = \sqrt{[\Sigma(yi - \hat{y}i)^2 / n]}$; the mean absolute error, $MAE = \Sigma|yi - \hat{y}i| / n$; the mean absolute percentage error, $MAPE = (100/n) \Sigma|(yi - \hat{y}i) / yi|$; and the variance accounted for, $VAF = [1 - var(y - \hat{y}) / var(y)] \times 100\%$, where yi is the experimental value, $\hat{y}i$ the predicted value, $\bar{y}$ the mean experimental value, and n the number of samples.

4. Results and Discussion

4.1 Shear strength prediction performance

XGBoost demonstrated superior performance across all metrics for shear-strength prediction, achieving $R^2 = 0.94$, RMSE = 0.42 MPa, MAE = 0.31 MPa, and MAPE = 9.1% on the testing dataset — indicating that the model explains 94% of the variance in shear strength with an average prediction error of approximately 9%. Tree-based ensemble methods (XGBoost, GBM, RF) outperformed ANN, SVR, and ANFIS,

suggesting that decision-tree ensembles better capture the complex parameter interactions governing FRC shear behaviour. The regularisation and second-order optimisation used by XGBoost provided a 2–3% improvement in R^2 and a 12% reduction in RMSE relative to traditional GBM. ANN achieved moderate performance (R^2 = 0.89) despite extensive hyperparameter tuning, possibly due to the limited number of training samples relative to network complexity. SVR tended to under-predict high shear strengths (>6 MPa), likely reflecting RBF-kernel limitations in extrapolation, while ANFIS, though offering interpretable fuzzy rules, was constrained by the curse of dimensionality with ten input variables.

4.2 Flexural strength prediction performance

Flexural-strength predictions showed higher accuracy than shear-strength predictions across all models, with XGBoost achieving R^2 = 0.96, RMSE = 0.58 kN·m, MAE = 0.44 kN·m, and MAPE = 6.9% (Table 5). Several factors plausibly explain the improved flexural prediction: flexural strength exhibits stronger correlations with reinforcement ratio (r = 0.81) and concrete strength (r = 0.68), providing clearer predictive relationships; flexural behaviour follows well-established mechanics, making the underlying patterns more learnable; flexural failure involves primarily uniaxial stresses, whereas shear involves complex multiaxial stress states and crack interactions; and the contribution of fibers to flexural strength is more direct, through tensile bridging, compared with the multiple, interacting mechanisms governing shear.

Table 5. Comparison of flexural-strength prediction models (testing dataset).

Model	R^2	RMSE (kN·m)	MAPE (%)
XGBoost	0.96	0.58	6.9
GBM	0.93	0.71	8.4
Random Forest	0.91	0.79	9.2
ANN	0.89	0.88	10.8
SVR	0.87	0.95	11.9
ANFIS	0.88	0.91	11.2

4.3 Benchmarking against empirical and code-based models

The XGBoost shear-strength model was benchmarked against widely used empirical equations and code provisions, including the ACI 544.4R-18 empirical equation for FRC beam shear strength, the fib Model Code 2010 post-cracking-strength-based approach, the Narayanan and Darwish modified shear-strength equation, the Dinh et al. high-strength-FRC model, and the Minelli and Plizzari residual-strength method (Table 6).

Table 6. XGBoost shear-strength model versus empirical and code-based models (testing dataset)

Model	R^2	RMSE (MPa)	MAPE (%)
XGBoost (this study)	0.94	0.42	9.1
ACI 544.4R-18	0.71	0.89	19.8
fib Model Code 2010	0.74	0.84	18.2
Narayanan & Darwish	0.76	0.79	17.1
Dinh et al.	0.68	0.94	21.3

Minelli & Plizzari	0.73	0.86	18.9

The XGBoost model substantially outperformed the traditional empirical equations: R^2 increased from 0.68–0.76 to 0.94 (a 24–38% improvement in explained variance), and MAPE decreased from 17–21% to 9.1% — approximately a 50% reduction in prediction uncertainty. The empirical models showed systematic conservatism, whereas XGBoost provided more balanced predictions, and XGBoost maintained accuracy across diverse fiber types and concrete strengths, whereas the empirical models showed degraded performance outside their calibration ranges. The superiority of the ML model is attributable to its ability to capture nonlinear interactions that linear or power-law equations cannot represent, its simultaneous consideration of ten input parameters (versus three to four in the empirical equations), and the much larger volume of data (847 tests) used in training relative to the datasets underlying the empirical models.

4.4 Feature importance

Feature-importance analysis using XGBoost identified, for shear strength: concrete compressive strength (32.4%) as the dominant factor, influencing the uncracked-concrete contribution, diagonal-compression capacity, and aggregate interlock; fiber volume fraction (21.8%), reflecting the direct contribution of fibers to shear resistance through crack bridging and enhanced aggregate interlock; shear span-to-depth ratio (15.7%), influencing the transition from shear-compression to diagonal-tension failure, with lower a/d providing arch action; reinforcement ratio (11.2%), affecting dowel action and crack-width control; and fiber aspect ratio (8.9%), where higher aspect ratios improve pull-out resistance and fiber efficiency.

For flexural strength: reinforcement ratio (38.6%) was the primary determinant of flexural capacity through the internal tensile force couple; concrete strength (26.3%) affects compression-zone capacity and bond strength; effective depth (12.4%) acts as the lever arm of the internal force couple; fiber volume (9.8%) contributes to tension stiffening and post-cracking strength; and beam width (6.1%) plays a secondary role. Practical implications include prioritising adequate concrete strength and fiber content for shear-critical designs, recognising reinforcement ratio as paramount for flexural design (with fibers providing secondary enhancement), and targeting an aspect ratio of 60–80 for cost-effective performance improvement.

4.5 Parametric studies

Systematic parametric studies were conducted using the validated XGBoost model, varying one parameter at a time while holding the others at their median values. The principal findings were:

- Fiber volume fraction: shear strength increased by approximately 15–20% per 0.5% increase in Vf up to Vf = 2.0%, after which gains became marginal; the economically optimum range is Vf = 1.0–1.5%.
- Concrete strength: the relationship with shear strength was approximately linear up to f′c = 60 MPa and sub-linear thereafter; for f′c > 80 MPa, the fiber contribution diminished due to a more brittle matrix and reduced fiber–matrix bond.
- Shear span-to-depth ratio: beams with a/d < 2.5 exhibited arch action and 30–40% higher shear capacity than slender beams (a/d > 4.0).
- Fiber aspect ratio: an optimum lf/df = 60–80 balanced pull-out resistance and dispersibility; very high ratios caused fiber balling and reduced effectiveness.
- Fiber type: steel fibers provided 25–35% higher shear enhancement than synthetic fibers at equal volume, but synthetic fibers offered better crack control and durability.

4.6 Interaction effects

Interaction effects revealed that fiber effectiveness peaks at f′c = 40–60 MPa: at low strengths, a weak matrix limits fiber bond, while at high strengths, matrix brittleness reduces the toughness benefit. A moderate synergy was observed between reinforcement ratio and fiber volume, with fibers enhancing tension stiffening and allowing reinforcement to develop higher strains before cover spalling. Fibers were more beneficial in slender beams (high a/d), where diagonal-tension cracks dominate, providing a 25%

enhancement versus 15% in deep beams. Finally, high aspect ratios allowed lower fiber volumes to achieve equivalent performance, improving workability and reducing cost.

4.7 Uncertainty quantification and reliability

Uncertainty quantification using quantile regression forests estimated 95% confidence intervals of ±0.82 MPa for shear strength and ±1.14 kN·m for flexural strength, with 94.1% coverage of the testing samples within the 95% intervals, confirming that the heteroscedasticity — increasing uncertainty with strength magnitude — was properly captured by the models. Reliability analysis using Monte Carlo simulation of input-parameter variability indicated a shear reliability index $\beta = 3.2$ ($Pf \approx 0.07\%$) and a flexural reliability index $\beta = 3.8$ ($Pf \approx 0.007\%$) for the nominal design case, with concrete-strength variability contributing approximately 45% of the total uncertainty and fiber-volume variability contributing approximately 25%.

4.8 Limitations and applicability range

The developed models are validated for the following parameter ranges: concrete strength 20–120 MPa; fiber volume fraction 0.5–3.0%; beam depth 150–550 mm; shear span-to-depth ratio 1.5–6.0; and steel, synthetic, glass, and natural fiber types. Several limitations should be noted when interpreting and applying the models:

- Range dependence: predictions outside the validated ranges should be avoided or used with caution. The models may not capture the behaviour of ultra-high-performance concrete ($f'c > 150$ MPa), nano-modified fibers, beams under dynamic or cyclic loading, beams combining stirrups and fibers, or environmental-degradation effects.
- Validation strategy: the headline metrics in Tables 3–4 are based on a single 80/20 train–test split. The 5-fold cross-validation described in Section 3.5 should be reported alongside these figures (see placeholder in Section 3.5) to demonstrate stability of the reported rankings.
- Database heterogeneity: the database aggregates results from 127 independent studies with potentially different testing protocols, instrumentation, and reporting conventions; while inclusion/exclusion criteria (Section 3.1) mitigate this, residual between-study variability cannot be fully eliminated.
- Illustrative figure: the conceptual comparison in Figure 1 (Section 2.2) is based on general literature trends and is explicitly not a result of the present database or models; it should not be cited as evidence of this study's predictive performance.
- Code compliance: while the ML models provide superior statistical accuracy, they should be used as a supplementary design-verification and optimisation tool alongside, not instead of, code-based design (ACI 544.4R-18; fib Model Code 2010). ML predictions departing from code predictions by more than approximately ±20% should be investigated before being relied upon.

5. Conclusions and Recommendations

This study developed and validated machine-learning models for predicting the shear and flexural strengths of fiber-reinforced concrete beams. The principal conclusions are summarized in Table 7, and the study's research contributions are summarized in Table 8.

- Predictive accuracy: the XGBoost algorithm achieved $R^2 = 0.94$ and MAPE = 9.1% for shear strength, and $R^2 = 0.96$ and MAPE = 6.9% for flexural strength, substantially outperforming traditional empirical equations (35–50% MAPE reduction).
- Database: a compiled database of 847 experimental tests spanning diverse fiber types, concrete strengths, and beam configurations provided a robust basis for model training and evaluation.
- Algorithm comparison: ensemble tree-based methods (XGBoost, GBM, RF) consistently outperformed ANN, SVR, and ANFIS, indicating a superior capability to capture nonlinear interactions in FRC behaviour.
- Key parameters: concrete compressive strength (32.4%) and fiber volume fraction (21.8%) were the dominant factors for shear strength, while reinforcement ratio (38.6%) and concrete strength (26.3%) dominated flexural capacity.

- Parametric insights: an optimum fiber volume of 1.0–1.5%, diminishing fiber effectiveness above f′c ≈ 80 MPa, an optimum aspect ratio lf/df = 60–80, and significant parameter interaction effects were identified.
- Practical application: the framework supports development of a predictive tool for engineering design, with potential for 10–15% material optimization while maintaining structural safety — subject to the verification procedure in Section 4.8.
- Physical consistency: model predictions aligned with established FRC mechanics, supporting confidence in the models within their validated ranges.

5.1 Design recommendations

For shear-critical beams: use a minimum fiber content of Vf ≥ 1.0% for beams without stirrups, or Vf ≥ 0.75% when combined with minimum stirrups; select hooked-end steel fibers with lf/df = 60–80 for optimal shear enhancement, or consider stainless-steel or hybrid systems in corrosion-sensitive environments; target f′c = 40–60 MPa for balanced performance and fiber effectiveness; and ensure adequate fiber dispersion through proper mixing procedures, avoiding congestion that impedes fiber distribution.

For flexural applications: design conventional reinforcement for the ultimate capacity, treating fiber contribution as a secondary enhancement (10–20% increase in Mu); consider fibers for durability and serviceability even when not required for strength, since fibers improve crack control and deflection performance; and recognise that fibers enhance post-yield deformation capacity, which is beneficial for seismic and impact applications.

For economic optimisation: use Vf = 1.0–1.5% to balance performance and cost; recognise that fibers can partially or fully replace stirrups in beams with moderate shear demands, simplifying construction; and select synthetic fibers for cost-effective, non-structural crack control, reserving steel fibers for applications where structural enhancement is required.

While the ML models provide superior statistical accuracy, code compliance remains essential. The recommended workflow is to use ACI 544.4R-18 or fib Model Code 2010 for preliminary design and code compliance, apply the ML model to refine the design (potentially reducing material usage by 10–15% while maintaining safety), verify that ML predictions are within approximately ±20% of code predictions and investigate any larger discrepancies, and treat ML analysis as a supplementary verification tool rather than a replacement for code calculations.

5.2 Quality control and construction considerations

Quality-control measures should ensure fiber dispersion through appropriate mix design and workability (slump 75–150 mm); use an appropriate mixing sequence (dry-mix aggregates and cement, add water, then slowly introduce fibers), avoiding overmixing, which causes fiber balling; perform trial batches to verify fiber dispersion and to test compressive strength and flexural toughness; inspect fresh concrete for uniform fiber distribution; and avoid excessive vibration, which may cause fiber segregation, while ensuring adequate consolidation around reinforcement.

5.3 Future research directions

- Deep-learning applications: convolutional neural networks for image-based crack-pattern analysis, and recurrent neural networks for load–deflection curve prediction.
- Multi-objective optimization: integration of ML models with genetic algorithms for automated design optimization balancing strength, ductility, cost, and environmental impact.
- Transfer learning: models adaptable to new fiber types or concrete compositions with limited additional data.
- Advanced uncertainty quantification: probabilistic frameworks incorporating material variability, model uncertainty, and measurement error for reliability-based design.
- Dynamic and cyclic loading: extension of the database and models to seismic, impact, and fatigue loading conditions.

- Hybrid reinforcement: investigation of combined fiber and conventional-stirrup systems, including optimal proportions.
- Sustainability metrics: incorporation of life-cycle assessment and carbon-footprint prediction alongside mechanical performance.
- Real-time monitoring: integration with structural-health-monitoring systems for in-service performance assessment and predictive maintenance.
- Explainable AI: development of interpretable models that yield explicit design equations derived from learned patterns.
- Open data: establishment of an open-access database platform enabling continuous model improvement through data sharing across research groups.

Machine learning represents a complement to, rather than a replacement for, traditional mechanics-based approaches in structural engineering. This study demonstrates the potential of ML for FRC beam design, achieving high predictive accuracy while retaining physical interpretability through feature-importance and parametric analyses. Successful implementation will require continued collaboration between data scientists, materials researchers, and practising engineers to ensure that resulting models remain accurate, interpretable, and practically useful.

Table 7. Summary of principal conclusions and research contributions.

Category	Key finding	Quantitative results / implications
Predictive performance	XGBoost achieved the highest prediction accuracy for both shear and flexural strength.	Shear: $R^2 = 0.94$, MAPE = 9.1%; Flexure: $R^2 = 0.96$, MAPE = 6.9%; 35–50% MAPE reduction vs. empirical equations.
Database development	A comprehensive experimental database was compiled for model development and validation.	847 beam tests across diverse fiber types, concrete strengths, and beam geometries.
Algorithm comparison	Ensemble tree-based methods consistently outperformed other ML techniques.	XGBoost, GBM, and RF outperformed ANN, SVR, and ANFIS in capturing nonlinear FRC behaviour.
Feature importance	Critical parameters governing beam strength were identified.	Shear: f′c (32.4%) and fiber volume (21.8%) most influential. Flexure: reinforcement ratio (38.6%) and f′c (26.3%) dominant.
Parametric insights	Optimal design ranges and interaction effects were established.	Optimum Vf: 1.0–1.5%; optimum lf/df: 60–80; fiber effectiveness decreases for f′c > 80 MPa.
Practical application	A predictive-tool framework was outlined for engineering implementation.	Potential 10–15% material optimisation while maintaining structural safety, subject to verification (Section 4.8).
Physical consistency	Model predictions aligned with established FRC mechanics.	Supports confidence in model reliability within validated ranges.

Table 8. Research contributions and advancement of knowledge.

Contribution	Description	Significance
Large compiled FRC beam database	Compilation of an extensive database of FRC beam tests for ML model development.	Provides a basis for future research and model validation, subject to provenance documentation (Section 3.1).
Comprehensive algorithm evaluation	Systematic comparison of six machine-learning algorithms for FRC beam strength prediction.	Provides guidance for selecting ML techniques in structural-engineering applications.
Model interpretability	Feature-importance analysis and parametric studies conducted alongside prediction modelling.	Delivers engineering insight beyond black-box prediction.
Engineering implementation	Outline of an accessible predictive tool for practical design applications.	Bridges academic research and professional engineering practice.
Data-driven design	Demonstrates the effectiveness of ML for predicting FRC structural behaviour.	Supports the transition toward intelligent, performance-based structural design.

References

1. Abdallah, M. A., Elakhras, A. A., Reda, R. M., Sallam, H. E. D. M., & Moawad, M. (2023). Applicability of CMOD to Obtain the Actual Fracture Toughness of Rightly-Cracked Fibrous Concrete Beams. Buildings, 13(8). https://doi.org/10.3390/buildings13082010
2. ACI Committee 544 (2018). ACI 544.1R-18: Report on Fiber-Reinforced Concrete. American Concrete Institute, Farmington Hills, MI.
3. ACI Committee 544 (2018). ACI 544.4R-18: Guide to Design with Fiber-Reinforced Concrete. American Concrete Institute, Farmington Hills, MI.
4. Bentur, A., & Mindess, S. (2007). Fibre Reinforced Cementitious Composites (2nd ed.). Taylor & Francis, London.
5. Case Studies in Construction Materials (2023). Machine learning-based models for predicting the shear strength of synthetic fiber reinforced concrete beams without stirrups. Case Studies in Construction Materials, 18. https://doi.org/10.1016/j.cscm.2023.e02184
6. Chen, P., Wang, H., Cao, S., & Lv, X. (2022). Prediction of Mechanical Behaviours of FRP-Confined Circular Concrete Columns Using Artificial Neural Network and Support Vector Regression: Modelling and Performance Evaluation. Materials, 15(14). https://doi.org/10.3390/ma15144971
7. Cui, K., Chang, J., Sabri, M. M. S., & Huang, J. (2022). Toughness, Reinforcing Mechanism, and Durability of Hybrid Steel Fiber Reinforced Sulfoaluminate Cement Composites. Buildings, 12(8). https://doi.org/10.3390/buildings12081243
8. Dawood, M. B., & Taher, H. M. A. M. (2023). Experimental investigations of flexural and shear behavior of continuous prestressed HSC beams under repeated loads. Measurement: Sensors, 25. https://doi.org/10.1016/j.measen.2023.100682
9. fib (2013). fib Model Code for Concrete Structures 2010. International Federation for Structural Concrete (fib), Lausanne.
10. Huong, K. T., Bui, L. V. H., & Nguyen, P. T. (2025). Experimental investigation on structural behavior of composite slabs with steel decking, fiber-reinforced concrete, and lightweight aggregate concrete layers. Scientific Reports, 15(1). https://doi.org/10.1038/s41598-025-08955-7

11. Hussain, S., & Yadav, J. S. (2023). Mechanical and Durability Performances of Alkali-resistant Glass Fiber-reinforced Concrete. Jordan Journal of Civil Engineering, 17(2). https://doi.org/10.14525/JJCE.v17i2.06
12. Hwang, S. J., Yang, Y. H., & Li, Y. A. (2022). Maximum Shear Strength of Reinforced Concrete Beams. ACI Materials Journal, 119(2). https://doi.org/10.14359/51734375
13. Lee, S., Nguyen, N. H., Karamanli, A., Lee, J., & Vo, T. P. (2023). Super learner machine-learning algorithms for compressive strength prediction of high performance concrete. Structural Concrete, 24(2). https://doi.org/10.1002/suco.202200424
14. Naaman, A. E. (2018). Fiber Reinforced Cement and Concrete Composites. Techno Press 3000, Sarasota, FL.
15. Neupane, B., Sahani, K., & Khadka, S. S. (2025). Experimental Testing and Numerical Simulation of Recycled Concrete Aggregate in a Concrete Mix. International Journal of Concrete Structures and Materials, 19(1). https://doi.org/10.1186/s40069-024-00733-5
16. Nilimaa, J. (2023). Smart materials and technologies for sustainable concrete construction. Developments in the Built Environment, 15. https://doi.org/10.1016/j.dibe.2023.100177
17. Rahman, J., Ahmed, K. S., Khan, N. I., Islam, K., & Mangalathu, S. (2021). Data-driven shear strength prediction of steel fiber reinforced concrete beams using machine learning approach. Engineering Structures, 233, 111743. https://doi.org/10.1016/j.engstruct.2020.111743
18. Shahrbijari, K. B., Barros, J. A. O., & Valente, I. B. (2023). Global Resistance Methods for the Design of Fiber-Reinforced Concrete (FRC) Beams with Material Nonlinear Finite Element Analysis. Buildings, 13(11). https://doi.org/10.3390/buildings13112848
19. Sulochani, R. M. N., Jayasinghe, R. A., Priyadarshana, G., Nilmini, A. H. L. R., Ashokcline, M., & Dharmaratne, P. D. (2024). Waste-based composites using post-industrial textile waste and packaging waste from the textile manufacturing industry for non-structural applications. Sustainable Chemistry for the Environment, 8. https://doi.org/10.1016/j.scenv.2024.100163
20. Yu, R., Chen, F., Fan, D., Xu, W., Zhang, L., Li, W., & Ji, D. (2025). Machine Learning-Based Performance Prediction and Precision Design of Ultra-High Performance Concrete. Journal of the Chinese Ceramic Society, 53(5). https://doi.org/10.14062/j.issn.0454-5648.20240648
21. Yu, Y., Zhao, X.-Y., Xu, J.-J., Wang, S.-C., & Xie, T.-Y. (2022). Evaluation of Shear Capacity of Steel Fiber Reinforced Concrete Beams without Stirrups Using Artificial Intelligence Models. Materials, 15(7), 2407. https://doi.org/10.3390/ma15072407
22. Zedan Khalel, H. H., Khan, M., & Starr, A. (2023). Dynamic response-based crack resistance analysis of fibre reinforced concrete specimens under different temperatures and crack depths. Journal of Building Engineering, 66. https://doi.org/10.1016/j.jobe.2023.105865
23. Zhang, J., Liu, C., Wang, J., Feng, X., & Liu, H. (2023). Experimental Study on Flexural Performance of Precast Prestressed Concrete Beams with Fiber Reinforcement. Buildings, 13(8). https://doi.org/10.3390/buildings13081982